

## CALL FOR PAPERS | *Oxygen Sensing: Life and Death of a Cell*

# Labeling of skeletal myoblasts with a novel oxygen-sensing spin probe for noninvasive monitoring of in situ oxygenation and cell therapy in heart

Sheik Wisel,<sup>1</sup> Simi M. Chacko,<sup>2</sup> M. Lakshmi Kuppusamy,<sup>2</sup> Ramasamy P. Pandian,<sup>2</sup>  
Mahmood Khan,<sup>2</sup> Vijay Kumar Kutala,<sup>2</sup> Richard W. Burry,<sup>3</sup> Benjamin Sun,<sup>1</sup>  
Pawel Kwiatkowski,<sup>1</sup> and Periannan Kuppusamy<sup>2</sup>

Center for Biomedical Electron Paramagnetic Resonance Spectroscopy and Imaging, <sup>1</sup>Division of Cardiothoracic Surgery, Department of Surgery; <sup>2</sup>Division of Cardiovascular Medicine, Department of Internal Medicine; and <sup>3</sup>Department of Neuroscience, Davis Heart and Lung Research Institute, The Ohio State University, Columbus, Ohio

Submitted 26 September 2006; accepted in final form 27 November 2006

**Wisel S, Chacko SM, Kuppusamy ML, Pandian RP, Khan M, Kutala VK, Burry RW, Sun B, Kwiatkowski P, Kuppusamy P.** Labeling of skeletal myoblasts with a novel oxygen-sensing spin probe for noninvasive monitoring of in situ oxygenation and cell therapy in heart. *Am J Physiol Heart Circ Physiol* 292: H1254–H1261, 2007. First published December 1, 2006; doi:10.1152/ajpheart.01058.2006.—We report the labeling (internalization) of skeletal myoblasts (SMs) with a novel class of oxygen-sensing paramagnetic spin probe for noninvasive tracking and in situ monitoring of oxygenation in stem cell therapy using electron paramagnetic resonance (EPR) spectroscopy. SM cells were isolated from thigh muscle biopsies of mice and propagated in culture. Labeling of SM cells with the probe was achieved by coincubating the cells with submicron-sized ( $270 \pm 120$  nm) particulates of the probe in culture for 48 h. The labeling had no significant effect on the viability or proliferation of the cells. The SM cells labeled with the probe were transplanted in the infarcted region of mouse hearts. The engraftment of the transplanted cells in the infarct region was verified by using MY-32 staining for skeletal myocytes. The in situ  $P_{O_2}$  in the heart was determined noninvasively and repeatedly for 4 wk after transplantation. The results showed significant enhancement of myocardial oxygenation at the site of cell transplant compared with untreated control. In conclusion, labeling of SM cells with the oxygen-sensing spin probe offers a unique opportunity for the noninvasive monitoring of transplanted cells as well as in situ tissue  $P_{O_2}$  in infarcted mouse hearts.

electron paramagnetic resonance spectroscopy; myocardial infarction; lithium octa-*n*-butoxy-naphthalocyanine; OxySpin

IN PATIENTS WITH myocardial infarction (MI) and congestive heart failure, stem cell treatment is being considered as a viable therapy for possible recovery of normal function of the heart. Studies using animal models have indicated that treatment of infarcted hearts with bone marrow-derived adult stem cells may regenerate the damaged myocardium and improve left ventricular function by inducing myogenesis and vasculogenesis (30). Some of the most recent data suggest that various types of lineage negative, c-kit positive ( $lin^-$  c-kit $^+$ ) bone marrow-derived cells (BMC), including hematopoietic stem/progenitor cells and mesenchymal cells, can repair damaged myocardium after MI and improve cardiac remodeling (27, 29, 43). Although the beneficial effects of stem cell therapy in humans have not been fully established,

several studies have shown that patients with acute MI treated with the BMC showed significant increase in left ventricular contractile function (1, 10, 36, 37, 40, 46). On the other hand, treatment with mononuclear BMC did not show any improvement (24). Thus the ideal cell type for effective cardiac repair and actuation of molecular mechanisms that mediate functional improvement is still to be determined.

Skeletal myoblast (SM) cells, because of their innate ability to propagate in large numbers, have become a potential choice for cardiac repair (31). The SM cells are easily isolated from skeletal muscle biopsies, amplified in culture, and transplanted in the infarcted region of the heart (2, 17, 19, 35, 41). A major limitation of using SM cell transplantation is the arrhythmic effects seen in some of the patients who received autologous SM cell transplantation (26, 39). However, this effect was not reported in animal studies (22, 28, 41). SM cell transplantation into the scar region but not in the border zone could prevent the occurrence of arrhythmias (11). There are a number of factors that have been shown to limit the expected therapeutic outcome of cell therapy. The major limiting factors are extensive loss of cells by washout, early cell death, and poor survival of the cell graft (14). The poor survival rate is attributed to the inflammatory reactions in the infarcted myocardium, deprivation of oxygen and nutrients, and mechanical injury caused by the implantation procedure (38).

In vivo monitoring, or the tracking of transplanted cells, is essential for a better understanding of their retention, migration, differentiation processes, and functional dynamics. Current strategies for cell-tracking use labeling with a thymidine analog [e.g., bromodeoxyuridine (BrdU)], or a transfected gene (e.g., green fluorescent protein or LacZ) for visualization using histochemical methods, optical imaging using bioluminescence and fluorescence, ultrasound, single-photon-emission computed tomography, and magnetic resonance imaging (MRI) using ultrasmall superparamagnetic particulates of iron oxide, have been shown to be useful for noninvasive cell tracking (6, 7, 9, 12, 16, 42). Unfortunately, the biodegradable nature of the probes limits long-term measurements (44). We report a novel class of oxygen-sensing paramagnetic spin probes that can be directly detected by electron paramagnetic resonance (EPR) spectroscopy.

Address for reprint requests and other correspondence: P. Kuppusamy, Davis Heart and Lung Research Inst., The Ohio State Univ., 420 W. 12th Ave., Rm. 114, Columbus, OH 43210 (e-mail: kuppusamy.1@osu.edu).

The costs of publication of this article were defrayed in part by the payment of page charges. The article must therefore be hereby marked "advertisement" in accordance with 18 U.S.C. Section 1734 solely to indicate this fact.

copy with high sensitivity and specificity (33). The probe, hereafter referred to as OxySpin, is made of submicron-sized crystals ( $270 \pm 120$  nm) of lithium octa-*n*-butoxynaphthalocyanine (LiNc-BuO) radicals (33). Our preliminary studies showed that a variety of mammalian cells can be labeled with OxySpin (34). Some of the unique features of OxySpin are substantially long-term biostability, nontoxicity, good cellular uptake (internalization), high sensitivity and specificity for EPR detection, and oxygen sensitivity. The cellular internalization and oxygen-sensing capability of the probe offers a unique advantage for studying stem cell therapy via noninvasive monitoring of transplanted cells and in situ oxygenation (PO<sub>2</sub>) in the treated region of hearts.

The purpose of this study was to develop procedures for the isolation and labeling of SM cells with OxySpin and to characterize the effects of the labeling on the toxicity, viability, proliferation, and function of the cells with an eventual goal of monitoring cell therapy in hearts in situ. The results clearly demonstrated the feasibility of labeling of SM cells with OxySpin and its potential to obtain substantially novel information during the process of cell engraftment.

## MATERIALS AND METHODS

**Isolation and purification of mouse SMs.** Skeletal muscle biopsies were excised from the hindlimb of mice under sterile conditions. The muscle specimens were immediately placed in a 10-cm tissue culture dish containing 10 ml of Hanks' balanced salt solution (HBSS, Invitrogen). After any bones, fat, connective tissue, or tendons were removed, the muscle biopsies were thoroughly minced into a fine slurry. The minced muscle was transferred to a 50-ml conical tube and centrifuged at 200 rpm for 3 min. The pellet was suspended in 3–4 ml of 0.2% collagenase type II (Worthington Biochemicals) in HBSS and incubated for 30 min at 37°C with constant shaking. The digested tissue was centrifuged for 5 min at 3,000 rpm. The pellet was resuspended in 3–4 ml of 0.25% trypsin-EDTA (Invitrogen) and incubated at 37°C for 30 min while constantly mixing. Ten milliliters of warm F-12 nutrient medium with 10% fetal bovine serum (FBS), 1% L-glutamine, and 1% antibiotic plus antimycotics (penicillin, streptomycin, and fungizone) (Invitrogen) were added. The digested tissue was triturated five times with 10 ml of growth medium using a pipette by drawing the mixture up and down inside the pipette repeatedly to break up any remaining pieces of muscle tissue and to release the muscle progenitor cells from beneath the basal lamina of the intact muscle fibers. After each trituration, the medium with cells was carefully transferred to a fresh 50-ml conical tube. The triturated medium was passed through a 100- $\mu$ m filter into a fresh 50-ml conical tube. The eluant from the filter was centrifuged at 3,000 rpm for 5 min, and the cell pellet was resuspended in 3 ml HBSS. The resuspended cells were loaded gently onto a Percoll gradient bed (40–70%, Sigma-Aldrich) and centrifuged at 2,500 rpm for 20 min at 25°C. The cells were removed from the interface of the 40–70% Percoll gradient and transferred to a fresh 50-ml conical tube. The cells were collected by centrifugation. The cells were counted with the use of a hemocytometer and then cultured in F-12 nutrient medium containing 20% FBS and 1% antibiotic/antimycotic agents.

**Flow cytometry.** Cells, after reaching 70–80% confluency, were trypsinized and checked for purity by flow cytometric analysis. Approximately  $1 \times 10^5$  cells were suspended in 145  $\mu$ l Dulbecco's phosphate-buffered saline (DPBS) containing 0.5% bovine serum albumin (BSA). The cells were stained with either isotype control antibody conjugated with FITC or with skeletal muscle-specific CD56 mouse monoclonal antibody conjugated with FITC (Pharmingen). The cells were mixed with the antibody and incubated for 1 h at 4°C. The cells were then centrifuged at 1,000 rpm for 10 min at room temperature. The

supernatants were decanted, and the pellet resuspended in 300  $\mu$ l DPBS containing 0.5% BSA and subjected to flow cytometry [fluorescence-activated cell sorting (FACS) analyzer, Beckman Coulter].

**Internalization (labeling) of OxySpin in skeletal myoblasts.** Microcrystalline particulates of lithium 5,9,14,18,23,27,32,36-octa-*n*-butoxy-2,3-naphthalocyanine (LiNc-BuO) were synthesized as reported (33). Approximately 10 mg of LiNc-BuO in 500  $\mu$ l of medium containing 5 mg of BSA were sonicated for a total of 7.5 min (using five cycles of 30-s sonication, followed by 1-min cooling on ice) to get uniform and smaller-sized ( $270 \pm 120$  nm) particulates using a probe sonicator (22.5 kHz, Sonic Dismembrator, Model 100, Fischer Scientific). A suspension of the sonicated particulates, diluted 20 $\times$  in DPBS, was sonicated for one more cycle and added to the cells. The cells were then incubated at 37°C in 5% CO<sub>2</sub> in an air-humidified environment. After 24, 48, or 72 h of incubation, the uninternalized particles in the medium were removed by washing two times with DPBS. The cells were then trypsinized, collected, and suspended in DPBS for analysis or transplantation.

**Cytotoxicity studies on myoblasts labeled with OxySpin.** SMs ( $1 \times 10^5$  cells) were cocultured with OxySpin (100  $\mu$ g/ml) for 48 h. After incubation, the cells were washed, trypsinized, and treated with Trypan blue. The number of live and dead cells was counted with the use of a hemacytometer. The viability of the cells was also measured by using a NucleoCounter (New Brunswick Scientific, Edison, NJ), an automated cell counter. This technique uses propidium iodide, which binds to cellular nuclei, and, depending on sample preparation, the counts provide the total number of cells or viable cells. Cytotoxicity was also determined by measuring the amount of lactate dehydrogenase (LDH) released in the cell culture medium using an optimized LDH procedure according to the manufacturer's instructions (Sigma). After incubation, an aliquot of the medium was taken and assayed for LDH activity using a Varian (model Cary 50) spectrophotometer at 340 nm at 25°C.

**Cell proliferation assay.** The effect of OxySpin on the proliferation of SM cells was evaluated by BrdU incorporation assay using the ELISA method according to the manufacturer's protocol (Colorimetric, Roche). Briefly, sonicated OxySpin particulates (100  $\mu$ g/ml) were added to cells (at 60–75% confluency) that were grown in 96-well plates, and the culture was then incubated for 48 h with gentle shaking every 6 h. BrdU (final concentration, 10  $\mu$ M) was added to each well and incubated overnight. The incorporated BrdU was detected by using a specific BrdU monoclonal antibody conjugated with peroxidase (1:100 dilution), followed by incubation with the substrate solution (tetramethylbenzidine). The peroxidase reaction was stopped by the addition of 25  $\mu$ l of 1 M sulfuric acid. Light absorbance at 450 nm (reference wavelength, 690 nm) was measured within 5 min using a microplate reader (Beckmann Coulter, AD 340). All experiments were run in at least three parallels and repeated three times.

**Oxygen consumption studies.** The effect of OxySpin labeling on cellular/mitochondrial function was assessed by measuring the cellular oxygen consumption using EPR spectroscopy (32). The labeled SM cells ( $1 \times 10^6$  cells/ml) were taken in a capillary tube (30  $\mu$ l), and both ends of the tube were then sealed. EPR measurements were performed by using a Bruker X-band (9.8 GHz) spectrometer (Bruker Instruments, Karlsruhe, Germany). In control experiments, OxySpin (10  $\mu$ g) was added externally to SM cells and the oxygen consumption was measured. EPR spectra were acquired for 30 min using custom-developed data acquisition software. Unless mentioned otherwise, the EPR line widths reported here are peak-to-peak widths ( $\Delta B_{pp}$ ) of the first derivative spectra. The oxygen consumption rates (OCRs) were determined from PO<sub>2</sub> data as a function of time.

**Animal preparation and induction of myocardial infarction.** C57BL male mice (weighing 25–30 g) were anesthetized with a mixture of ketamine (55 mg/kg) and xylazine (15 mg/kg) that was injected intraperitoneally. The intubation tube was made of a 20-gauge intravenous catheter attached to a connector. A modified Y-shaped connector was used to attach the mouse to the ventilator. The ventilator

was set at a rate of 120 breaths/min with a tidal volume of 250  $\mu$ l (Harvard Apparatus, Holliston, MA). The body temperature of the mice was maintained at  $37 \pm 1^\circ\text{C}$  with the help of an isothermal heating pad (Braintree Scientific, Braintree, MA). All of the procedures were performed with approval of the Institutional Animal Care and Use Committee of the Ohio State University and conformed to the *Guide for the Care and Use of Laboratory Animals* (National Institutes of Health Publication No. 86-23, Revised 1996).

MI in the mice was created by permanently occluding the left coronary artery (LCA) using the following procedure. An oblique 8-mm incision was made 2 mm away from the left sternal border toward the left armpit. The chest cavity was opened with scissors by a small incision (5 mm in length) at the level of the third or fourth intercostal space 2–3 mm from the left sternal border. The LCA was visualized as a pulsating bright red spike running through the midst of the heart wall from underneath the left atrium toward the apex. The LCA was ligated 1–2 mm below the tip of the left auricle using a tapered needle and an 8-0 polypropylene ligature passed underneath the LCA, and a double knot was made to occlude the LCA. Occlusion was confirmed by the dramatic change in color (pale) of the anterior wall of the left ventricle. The chest cavity was closed by bringing together the third and fourth ribs with one 6-0 polypropylene silk suture. The layers of muscle and skin were closed with a 5-0 polypropylene suture.

**Transplantation of skeletal myoblasts in the infarcted heart.** SMs ( $1 \times 10^5$  cells in 15  $\mu$ l medium) were implanted in the heart immediately after the ligation of the LCA. The cells were injected as a single dose into the midventricular region using a 29.5-gauge needle. The chest was closed after implantation of the cells, and EPR measurements were performed immediately and then every week for 4 wk using an L-band EPR spectrometer (Magnettech).

**In vivo measurements of  $PO_2$  in the heart.** The sensitivity of the EPR line width of OxySpin to oxygen was calibrated as described previously (33). The calibration curve of the EPR line width versus  $PO_2$  was linear with a sensitivity of 9.8 mG/mmHg. The mouse was placed in the EPR system with its heart close to the loop of the surface coil resonator. EPR spectra were acquired as single scans. The instrument settings were microwave power (4 mW), modulation

amplitude (180 mG), modulation frequency (100 kHz), receiver time constant (0.2 ms), and acquisition time (30 s). The peak-to-peak line width of the EPR spectrum was used to calculate  $PO_2$  using the standard calibration curve.

**Immunostaining with skeletal myosin-specific MY-32 antibody.** The differentiation of the transplanted SMs into skeletal muscle cells was identified using MY-32 staining. Mice were euthanized, and their hearts were removed either 1 or 4 wk after transplantation. The hearts were fixed in formalin and embedded in paraffin, and 4- $\mu$ m sections were then obtained. The sections were deparaffinized in xylene and rehydrated in a graded alcohol series. The sections were then incubated with the MY-32 primary antibody (Sigma, St. Louis, MO) (1:300 dilution) for 12 h, followed by incubation with the secondary antibody (1:2,000 dilution) for 1 h. Immunostaining was carried out at  $4^\circ\text{C}$ . The cells were examined for positive MY-32 staining to indicate the presence of SMs.

**Data analysis.** The statistical significance of the results was evaluated using ANOVA and Student's *t*-test. The values were expressed as means  $\pm$  SD. A *P* value  $<0.05$  was considered significant.

## RESULTS

**Isolation and characterization of SM cells.** SM cells isolated from the hindlimb skeletal muscle biopsies were grown in F-12 nutrient medium containing 20% FBS and 1% antibiotic/antimycotic agents (Fig. 1A). The SM cells appeared as spindle-shaped single cells in culture (Fig. 1B). The cells were not allowed to grow to confluency because they then tend to form myotubes (31). Therefore, the cell growth was limited to 60–70% confluency for the first three passages. At this stage, the cells were trypsinized and passed on to the next generation or used for experiments. At the end of three passages, the cells were stained for CD56, a marker specific for skeletal muscle (26), and their purity was determined by using flow cytometry. The purity of the SM cells, assessed by this procedure, was  $72 \pm 6\%$  (Fig. 1, C and D).

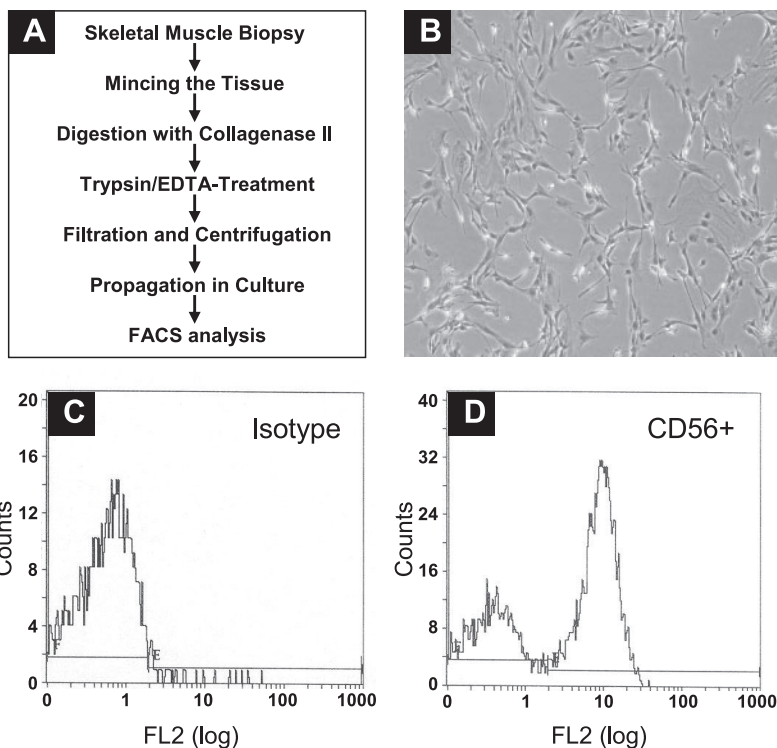


Fig. 1. Isolation and characterization of mouse skeletal myoblasts (SMs). *A*: steps in the isolation, purification, and propagation of SMs. *B*: representative optical micrograph of SMs in culture ( $\times 40$ ). *C* and *D*: flow cytometric analyses of purified SMs. The cells were stained with IgG $_{1\kappa}$  (nonspecific, isotype control; *C*) and CD56 (*D*) antibody, which is specific to a surface protein expressed by the SMs. The purity of SMs was  $72 \pm 6\%$ . FACS, fluorescence-activated cell sorting.

**Labeling of SM cells with OxySpin.** Labeling of SM cells was performed by adding OxySpin to the culture medium at concentrations of 60–200  $\mu\text{g/ml}$  and incubation periods of 24, 48, or 72 h. The results showed that SM cells can be efficiently labeled with OxySpin, presumably by endocytosis (Fig. 2). The efficiency of labeling by incubation of the SM cells with 100  $\mu\text{g/ml}$  of OxySpin for 48 h was manually determined by measuring the average of the number of labeled cells per field with an optical microscope and was observed to be  $>85\%$ . The EPR spectrum obtained from the labeled cells in suspension showed an intense single peak (Fig. 3A) characteristic of the OxySpin (33). The line width, measured as the peak-to-peak width of the derivative signal, was 1,980 mG in a room air-equilibrated suspension. The effect of oxygen tension in the solution (measured as the partial pressure of oxygen,  $P_{O_2}$ ) on the EPR line width of the labeled cells was determined by and compared with that of the probe only. The results, as shown in Fig. 3B, showed a linear dependence of the line width in both cases as a function of  $P_{O_2}$  in the range 0–250 mmHg ( $\sim 33\% O_2$ ). The oxygen sensitivity was  $9.8 \pm 0.1$  mG/mmHg. Furthermore, there was no significant difference between the oxygen sensitivities of the free probe and labeled cells, suggesting that the oxygen sensitivity of the probe was not altered upon its internalization in cells. We further studied the labeling efficiency by quantifying the amount (number of spins) of OxySpin in cells using EPR spectrometry. The SM cells ( $1 \times 10^6$ ) were incubated with various doses of OxySpin (60, 100, or 200  $\mu\text{g/ml}$ ) and incubated for 24, 48, or 72 h. The results, shown in Fig. 3, C and D, indicated that an optimum uptake of

OxySpin by SM cells was achieved by using a 48-h incubation of cells with 100  $\mu\text{g/ml}$  OxySpin. The rather large error bar in the uptake data is attributed to the heterogeneous nature of the distribution and contact of OxySpin particulates with cells in culture. Under these conditions, a mean value of  $\sim 3 \times 10^{10}$  spins/cell was achievable. It should be noted that this value is an order of magnitude higher than the detection sensitivity of typical X-band (in vitro) EPR spectrometers, suggesting that the probe can be detected from a single cell.

We carried out in vitro assays on OxySpin-labeled SM cells to examine cellular toxicity and proliferation. The results of cell viability assays by the Trypan blue exclusion method (Fig. 4A) and an automated NucleoCounter (Fig. 4B) and the release of LDH in the cell culture supernatants (Fig. 4C) revealed no apparent cytotoxicity in labeled cells compared with that in control. Also, the assay of BrdU incorporation in DNA did not show any significant effect of OxySpin/labeling on cell proliferation (Fig. 4D). Overall, the results showed that labeling had no significant adverse effects on the SM cells.

**Measurement of cellular oxygenation and consumption rate.** Cellular oxygen utilization is a measure of mitochondrial function. To investigate whether the labeling could alter cellular oxygen consumption, we measured the OCR in control and labeled SM cells. As shown in Fig. 5A, the OCRs of control and labeled cells were  $2.6 \pm 1.1$  and  $2.1 \pm 0.6$   $\text{nmol} \cdot \text{min}^{-1} \cdot 10^6 \text{ cells}^{-1}$ , respectively. The OCR results, along with the negligible rate observed in cells treated with cyanide, clearly established the mitochondrial utilization of the oxygen and that there was no significant difference in the OCR between labeled and control cells.

In cell therapy using the labeled cells, it is possible that the probes may come off or may be leached out in case of cell death. Hence, it is important to establish whether the intracellular  $P_{O_2}$  value obtained using the internalized OxySpin is comparable with the extracellular measurements. To do this, we measured the intracellular  $P_{O_2}$  in OxySpin-labeled cells equilibrated with room air (21%  $O_2$ ) or 5%  $O_2$  (balance nitrogen). The corresponding extracellular  $P_{O_2}$  values were obtained by adding large particulates ( $>5 \mu\text{m}$ ) of OxySpin to a suspension of control cells. The results (Fig. 5B) indicated a small decrease in the intracellular oxygenation compared with extracellular oxygenation in viable cells. However, the decrease was not statistically significant. The fact that the decrease was not due to the intracellular placement of the probe was confirmed by measurements taken after arresting mitochondrial respiration using cyanide poisoning.

**Noninvasive monitoring of cells and in situ  $P_{O_2}$  in infarcted hearts transplanted with labeled SM cells.** We further performed in vivo experiments to demonstrate the feasibility of making noninvasive measurements of  $P_{O_2}$  in infarcted mouse hearts transplanted with OxySpin-labeled SM cells. Myocardial infarction was induced by ligation of the LCA in mice. Immediately after ligation, a single injection of labeled SM cells ( $1 \times 10^5$  cells in 15  $\mu\text{l}$ ) was administered in the ischemic/infarct region. The retention, proliferation, and differentiation of the transplanted cells in the infarcted heart were examined by histochemical (hematoxylin-eosin) and immunohistochemical (MY-32, a skeletal muscle-specific myosin heavy chain marker) staining. Figure 6, A–D, shows the differentiation of the SM cells to SMs 1 wk after transplantation. The myocardial  $P_{O_2}$  was monitored regu-

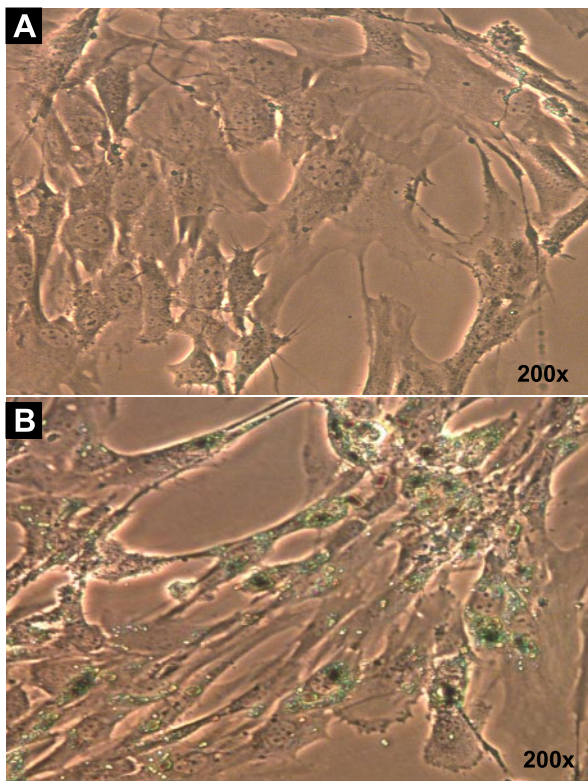
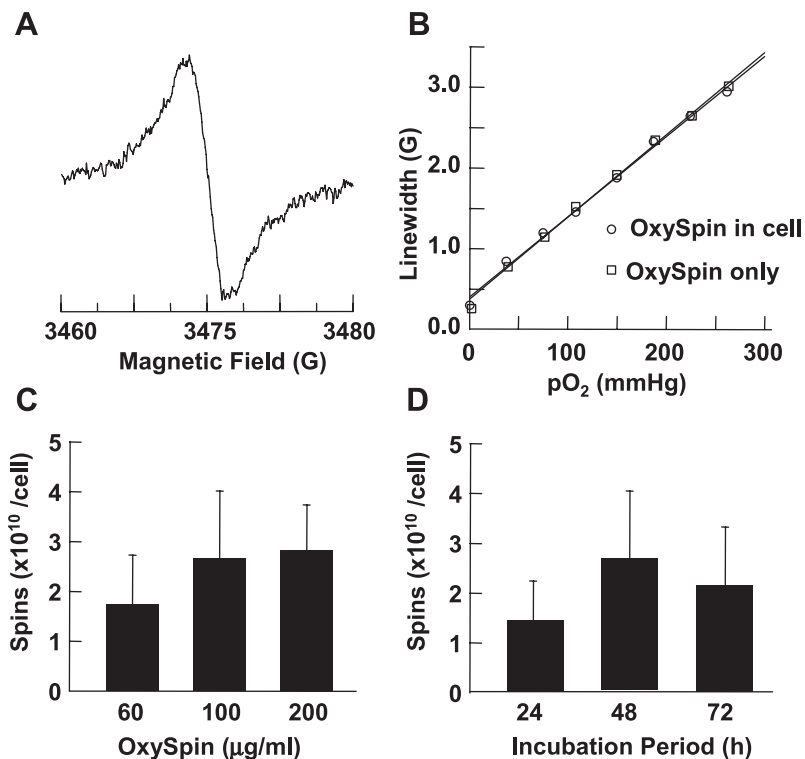


Fig. 2. SMs labeled with OxySpin. A: representative optical micrograph of SMs ( $\times 200$ ). B: SMs labeled with OxySpin ( $\times 200$ ). The labeling was performed by coculturing SMs with OxySpin (100  $\mu\text{g/ml}$ ) for 48 h. The internalized OxySpins are visible as dark-green stains.

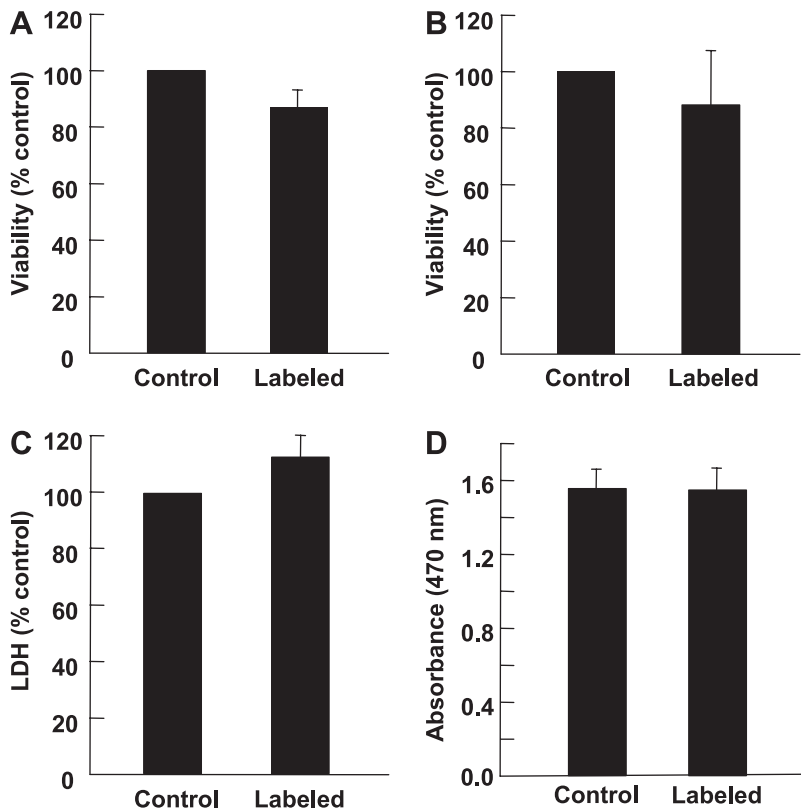
Fig. 3. Characterization of OxySpin internalized in SMs. *A*: a typical electron paramagnetic resonance (EPR) spectrum obtained from a suspension of labeled cells equilibrated with room air. The peak-to-peak line width of the EPR spectrum was 1.980 G. *B*: oxygen calibration of OxySpin in PBS and OxySpin internalized in SM showing a linear variation of line width with PO<sub>2</sub>. *C*: dose effect of OxySpin on the uptake by SM measured after 48 h of coincubation. *D*: effect of incubation time on the uptake of OxySpin by SM using a dose of OxySpin was 100 μg/ml. Data were obtained from 3 independent experiments and expressed as means ± SD. The results indicate that an optimum uptake of OxySpin by SM cells is achieved with a dose of 100 μg/ml at 48-h coincubation.



larly from the OxySpin-labeled cells at the site of implantation using in vivo EPR spectroscopy. Figure 6E shows the mean PO<sub>2</sub> values obtained from three groups of hearts at 4 wk after cell transplantation: control (no LCA ligation), ischemic (LCA ligation), and treated (LCA ligation fol-

lowed by SM treatment) hearts. It is seen that the mean PO<sub>2</sub> value in the treated group was significantly higher (*P* < 0.05) compared with that of the untreated ischemic group. The results clearly demonstrated the feasibility of the in vivo tracking of SMs labeled with oxygen-sensing spin

Fig. 4. Effect of OxySpin labeling on the viability and proliferation of SMs. SMs were coincubated with OxySpin (100 μg/ml) for 48 h. *A*: viability of SMs measured by trypan blue exclusion. *B*: cell viability measured by automated nuclear counter. *C*: lactate dehydrogenase (LDH) activity measured in the cell culture supernatants. *D*: bromodeoxyuridine cell proliferation assay performed by using 96-well plates as per the procedure described in MATERIALS AND METHODS. Data represent means ± SD obtained from 3 independent experiments. The control experiments did not include OxySpin in the culture.



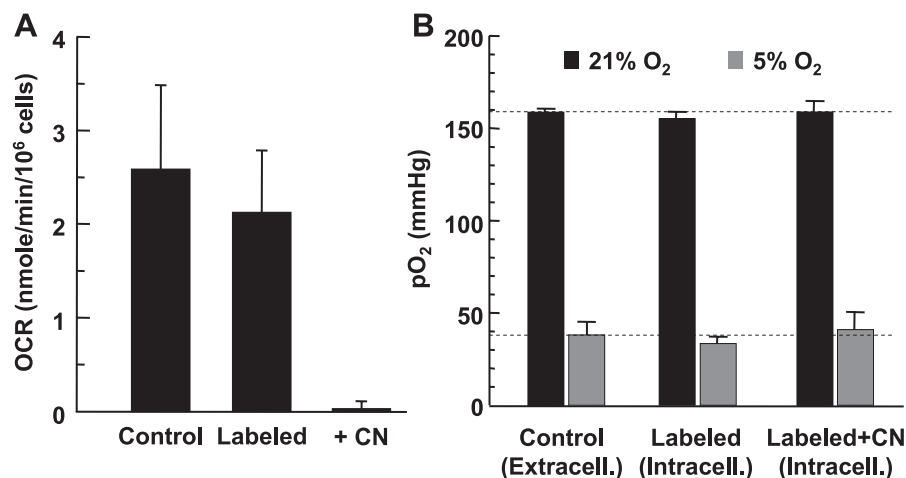


Fig. 5. Effect of OxySpin labeling on cellular oxygenation and consumption. *A*: oxygen consumption rate (OCR) of SMs labeled with OxySpin was measured by using EPR spectroscopy in a 20- $\mu$ l capillary tube containing 20,000 cells. *B*: extracellular (extracell) and intracellular (intracell) Po<sub>2</sub> values obtained, respectively, from control and labeled cells in suspension equilibrated with 21% or 5% oxygen. The measurements in control cells were performed by using externally added large-sized OxySpin particulates. Cyanide (CN, 100  $\mu$ M) was used to arrest mitochondrial respiration and oxygen utilization. Data are means  $\pm$  SD from 3 independent experiments. The results show that the labeling has no significant effect on the cellular oxygenation and OCR.

probes and monitoring changes in the myocardial tissue Po<sub>2</sub> in mice with MI.

**DISCUSSION**

The present study was designed to 1) label skeletal myoblast cells with the novel OxySpin probes for tracking

cells and monitoring oxygenation at the site of transplantation and 2) demonstrate the feasibility of cell-tracking and in situ measurement of oxygenation in the infarcted heart treated with cell transplantation using in vivo EPR spectroscopy. We used SMs isolated from mouse thigh muscle biopsies. These cells retain their characteristic fea-

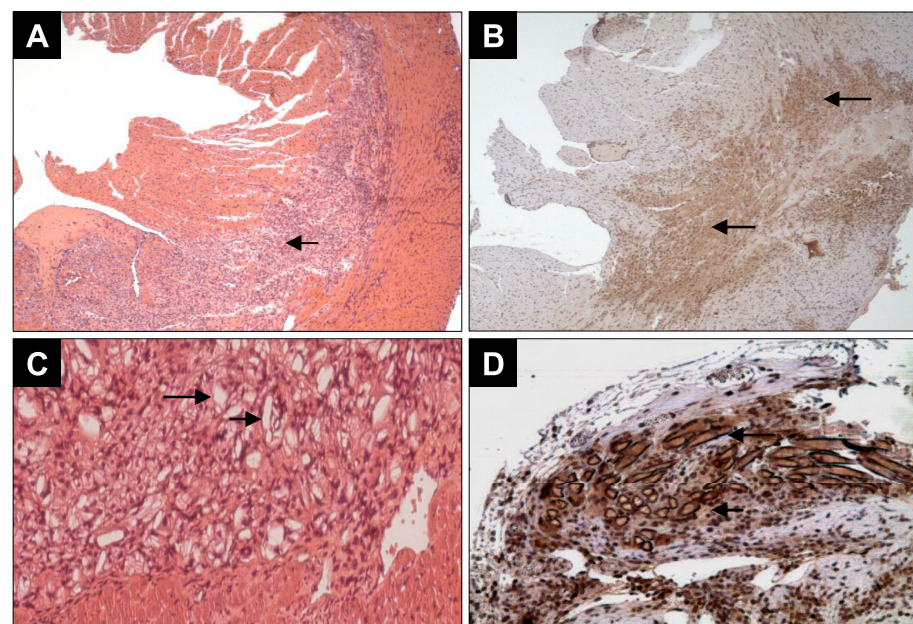
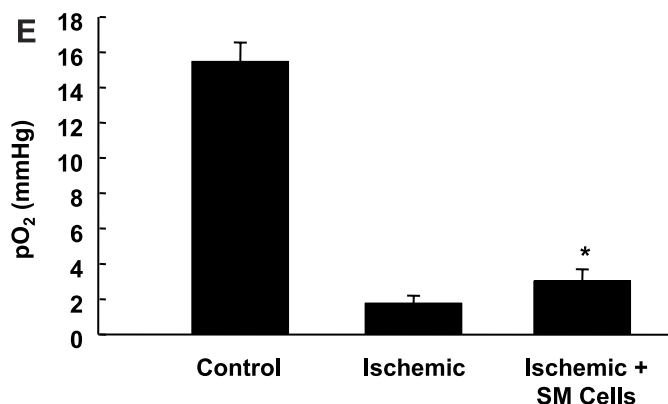


Fig. 6. Histological assessment and tissue oxygenation of the infarcted heart treated with SM transplantation. Myocardial infarction was created by ligation of left coronary artery (LCA) in mice. A single intramyocardial injection of labeled SM ( $1 \times 10^5$  cells in 15  $\mu$ l) was performed. Representative histochemical [hematoxylin-eosin (H&E)] and immunohistochemical (MY-32, a skeletal muscle-specific myosin heavy chain marker) stainings of heart sections obtained at 1 and 4 wk after transplantation with SM cells are shown. *A*: H&E staining: 1 wk,  $\times 4$ . *B*: MY-32 staining: 1 wk,  $\times 4$ . *C*: H&E staining: 2 wk,  $\times 100$ . *D*: MY-32 staining: 4 wk;  $\times 100$ . *A* and *B*, arrows: SM cells differentiated into SMs (brown color). *C*, arrows: presence of OxySpin (white color). *E*: mean Po<sub>2</sub> values obtained from 3 groups of hearts at 4 wk after cell transplantation: control (no LCA ligation), ischemic (LCA artery ligation), and treated (LCA ligation followed by SM treatment) hearts. Data are expressed as means  $\pm$  SD ( $n = 5$  animals/group,  $*P < 0.05$ ). The mean Po<sub>2</sub> value in the treated group was significantly higher compared with that of the untreated ischemic group.



ture of CD56 expression on their surfaces for up to 15 passages (31).

The results of the present study showed that SM cells can be efficiently labeled with OxySpin. The microscopic appearance of OxySpin-labeled SM cells did not differ from that of unlabeled SM cells. The mechanism of uptake of OxySpin is not yet known. However, we believe that the lipophilicity of the OxySpin particulates may contribute to their endocytosis in cells. Our studies revealed that optimal labeling could be achieved with 100 µg/ml of OxySpin coincubated with cells for 48 h. We determined the EPR spin density of OxySpin in cells by EPR spectroscopy to be  $2.5 \times 10^{10}$  spins/cell, which is an order of magnitude higher, compared with the detection limit of typical X-band EPR spectrometers. Thus it is possible to detect single cells by X-band EPR spectroscopy.

Previously, we demonstrated the labeling of OxySpin in different cell types, including endothelial cells, macrophages, smooth muscle cells, and cancer cells (21, 34). The time required for the labeling of OxySpin for these cells varied from 4 to 72 h of coincubation. We also observed that the EPR properties and oxygen sensitivity of OxySpin were not altered upon labeling. The toxicity studies clearly established that labeling has no significant effects on the SM cells. The results also showed that there was no significant difference in the OCR between labeled cells and controls, suggesting that labeling of cells with OxySpin did not alter the mitochondrial/cellular function, and thus the mitochondrial integrity was maintained.

Cell-based therapies pose a great challenge and limitation for the noninvasive monitoring of transplanted cells due to limited stem cell survival and engraftment (20). Hence, it is highly desirable to develop methods to noninvasively monitor the homing, engraftment, proliferation, or differentiation process after cellular transplantation to understand the stem cell response in the host tissue. The conventional method for the analysis of myocardial cell transplant and graft survival depends on postmortem histology (18). In a rat model of coronary occlusion, the efficacy of myoblast implantation was demonstrated by ex vivo histological staining procedures (28). Genetic markers, such as green fluorescent protein and LacZ, have been used as fluorescent labels for cell transplant studies (16, 42). Recently, CD34<sup>+</sup> cells labeled with Cell-Tracker Orange were injected into mice and were tracked in vivo for expression of neural antigens (13). There is a rapid growth in the use of MRI for cellular and molecular imaging to track stem cells after transplantation (4, 6–9, 15). However, all these methods have certain limitations, e.g., the analysis needs to be performed in excised samples, and functional parameters, such as cellular/tissue oxygenation, cannot be obtained. Results of the present study have clearly indicated the feasibility of the monitoring of transplanted SM cells and the measurement of local tissue PO<sub>2</sub> up to 4 wk after transplantation noninvasively by EPR spectroscopy. EPR signal was detected up to 4 wk after labeled SM cell transplantation, and the histological studies show the engraftment and differentiation of SM cells. Four weeks after the SM transplantation, the mean PO<sub>2</sub> value in the SM cell-treated group was significantly higher compared with that of the untreated ischemic group.

It should be noted that the timing of stem cell implantation with respect to the timing of induction of ischemic injury (MI) is also very critical for the efficacy of the therapy in animal models (23, 25, 45) as well as in human (3). We injected the

SMs immediately after LCA ligation. Because of the very high mortality rate, we avoided a second surgical procedure in mice to inject the cells after 1 or more wk following the creation of MI. This is indeed a limitation with the mice model of MI. We are currently investigating the effect of treatment timing on the therapeutic outcome using rat models of MI.

In conclusion, we have demonstrated for the first time the use of a novel bifunctional paramagnetic spin probe for the labeling and tracking of SMs in cell therapy. The labeling does not alter the cell viability or proliferation. We have further demonstrated the feasibility of the in vivo tracking of SMs and the determination of oxygen concentration from the engrafted site of infarcted hearts of mice. The labeling of stem cells with the oxygen-sensing spin probes offers a unique opportunity for the noninvasive monitoring of transplanted cells as well as in situ tissue PO<sub>2</sub> using EPR spectroscopy.

#### ACKNOWLEDGMENTS

We are grateful to Dr. Robert E. Michler for advice on cell therapy, Dr. Narasimham L. Parinandi for help with the labeling of cells, and Nancy Trigg for critical reading of the manuscript. V. K. Kutala was on sabbatical from Nizam's Institute of Medical Sciences, Hyderabad, India.

#### GRANTS

This study was supported by National Institutes of Health Grant R01-EB-004031 and a State of Ohio Third Frontier grant Biomedical Research and Technology Transfer/Cardiovascular Bioenterprise.

#### REFERENCES

1. Assmus B, Honold J, Schachinger V, Britten MB, Fischer-Rasokat U, Lehmann R, Teupe C, Pistorius K, Martin H, Abolmaali ND, Tonn T, Dimmeler S, Zeiher AM. Transcatheter transplantation of progenitor cells after myocardial infarction. *N Engl J Med* 355: 1222–1232, 2006.
2. Atkins BZ, Hueman MT, Meuchel JM, Cottman MJ, Hutcheson KA, Taylor DA. Myogenic cell transplantation improves in vivo regional performance in infarcted rabbit myocardium. *J Heart Lung Transplant* 18: 1173–1180, 1999.
3. Bartunek J, Wijns W, Heyndrickx GR, Vanderheyden M. Timing of intracoronary bone-marrow-derived stem cell transplantation after ST-elevation myocardial infarction. *Nat Clin Pract Cardiovasc Med* 3, Suppl 1: S52–S56, 2006.
4. Bos C, Delmas Y, Desmouliere A, Solanilla A, Hauger O, Grosset C, Dubus I, Ivanovic Z, Rosenbaum J, Charbord P, Combe C, Bulte JW, Moonen CT, Ripoché J, Grenier N. In vivo MR imaging of intravascularly injected magnetically labeled mesenchymal stem cells in rat kidney and liver. *Radiology* 233: 781–789, 2004.
5. Bulte JW, Douglas T, Witwer B, Zhang SC, Lewis BK, van Gelderen P, Zywicke H, Duncan ID, Frank JA. Monitoring stem cell therapy in vivo using magnetodendrimers as a new class of cellular MR contrast agents. *Acad Radiol* 9, Suppl 2: S332–S335, 2002.
6. Bulte JW, Duncan ID, Frank JA. In vivo magnetic resonance tracking of magnetically labeled cells after transplantation. *J Cereb Blood Flow Metab* 22: 899–907, 2002.
7. Bulte JW, Zhang SC, van Gelderen P, Herynek V, Jordan EK, Janssen CH, Duncan ID, Frank JA. Magnetically labeled glial cells as cellular MR contrast agents. *Acad Radiol* 9, Suppl 1: S148–S150, 2002.
8. Cahill KS, Gaidosh G, Huard J, Silver X, Byrne BJ, Walter GA. Noninvasive monitoring and tracking of muscle stem cell transplants. *Transplantation* 78: 1626–1633, 2004.
9. Drexler H, Meyer GP, Wollert KC. Bone-marrow-derived cell transfer after ST-elevation myocardial infarction: lessons from the BOOST trial. *Nat Clin Pract Cardiovasc Med* 3, Suppl 1: S65–S68, 2006.
10. Fouts K, Fernandes B, Mal N, Liu J, Laurita KR. Electrophysiological consequence of skeletal myoblast transplantation in normal and infarcted canine myocardium. *Heart Rhythm* 3: 452–461, 2006.
11. Frank JA, Miller BR, Arbab AS, Zywicke HA, Jordan EK, Lewis BK, Bryant LH Jr, Bulte JW. Clinically applicable labeling of mammalian and stem cells by combining superparamagnetic iron oxides and transfection agents. *Radiology* 228: 480–487, 2003.

13. Goolsby J, Marty MC, Heletz D, Chiappelli J, Tashko G, Yarnell D, Fishman PS, Dhib-Jalbut S, Bever CT Jr, Pessac B, Trisler D. Hematopoietic progenitors express neural genes. *Proc Natl Acad Sci USA* 100: 14926–14931, 2003.
14. Gussoni E, Blau HM, Kunkel LM. The fate of individual myoblasts after transplantation into muscles of DMD patients. *Nat Med* 3: 970–977, 1997.
15. Hill JM, Dick AJ, Raman VK, Thompson RB, Yu ZX, Hinds KA, Pessanha BS, Guttman MA, Varney TR, Martin BJ, Dunbar CE, McVeigh ER, Lederman RJ. Serial cardiac magnetic resonance imaging of injected mesenchymal stem cells. *Circulation* 108: 1009–1014, 2003.
16. Hoehn M, Kustermann E, Blunk J, Wiedermann D, Trapp T, Wecker S, Focking M, Arnold H, Hescheler J, Fleischmann BK, Schwandt W, Buhle C. Monitoring of implanted stem cell migration in vivo: a highly resolved in vivo magnetic resonance imaging investigation of experimental stroke in rat. *Proc Natl Acad Sci USA* 99: 16267–16272, 2002.
17. Hutcheson KA, Atkins BZ, Hueman MT, Hopkins MB, Glower DD, Taylor DA. Comparison of benefits on myocardial performance of cellular cardiomyoplasty with skeletal myoblasts and fibroblasts. *Cell Transplant* 9: 359–368, 2000.
18. Jackson KA, Majka SM, Wang H, Pocius J, Hartley CJ, Majesky MW, Entman ML, Michael LH, Hirschi KK, Goodell MA. Regeneration of ischemic cardiac muscle and vascular endothelium by adult stem cells. *J Clin Invest* 107: 1395–1402, 2001.
19. Jain M, DerSimonian H, Brenner DA, Ngoy S, Teller P, Edge AS, Zawadzka A, Wetzel K, Sawyer DB, Colucci WS, Apstein CS, Liao R. Cell therapy attenuates deleterious ventricular remodeling and improves cardiac performance after myocardial infarction. *Circulation* 103: 1920–1927, 2001.
20. Kalka C, Masuda H, Takahashi T, Kalka-Moll WM, Silver M, Kearney M, Li T, Isner JM, Asahara T. Transplantation of ex vivo expanded endothelial progenitor cells for therapeutic neovascularization. *Proc Natl Acad Sci USA* 97: 3422–3427, 2000.
21. Kutala VK, Parinandi NL, Pandian RP, Kuppusamy P. Simultaneous measurement of oxygenation in intracellular and extracellular compartments of lung microvascular endothelial cells. *Antioxid Redox Signal* 6: 597–603, 2004.
22. Leobon B, Garcin I, Menasche P, Vilquin JT, Audinat E, Charpak S. Myoblasts transplanted into rat infarcted myocardium are functionally isolated from their host. *Proc Natl Acad Sci USA* 100: 7808–7811, 2003.
23. Li RK, Mickle DA, Weisel RD, Rao V, Jia ZQ. Optimal time for cardiomyocyte transplantation to maximize myocardial function after left ventricular injury. *Ann Thorac Surg* 72: 1957–1963, 2001.
24. Lunde K, Solheim S, Aakhus S, Arnesen H, Abdelnoor M, Egeland T, Endresen K, Ilebakk A, Mangschau A, Fjeld JG, Smith HJ, Taraldsrud E, Groggaard HK, Bjornerheim R, Brekke M, Muller C, Hopp E, Ragnarsson A, Brinchmann JE, Forfang K. Intracoronary injection of mononuclear bone marrow cells in acute myocardial infarction. *N Engl J Med* 355: 1199–1209, 2006.
25. Ma J, Ge J, Zhang S, Sun A, Shen J, Chen L, Wang K, Zou Y. Time course of myocardial stromal cell-derived factor 1 expression and beneficial effects of intravenously administered bone marrow stem cells in rats with experimental myocardial infarction. *Basic Res Cardiol* 100: 217–223, 2005.
26. Menasche P, Hagege AA, Vilquin JT, Desnos M, Abergel E, Pouzet B, Bel A, Sarateanu S, Scorsin M, Schwartz K, Bruneval P, Benbunan M, Marolleau JP, Duboc D. Autologous skeletal myoblast transplantation for severe postinfarction left ventricular dysfunction. *J Am Coll Cardiol* 41: 1078–1083, 2003.
27. Min JY, Sullivan MF, Yang Y, Zhang JP, Converso KL, Morgan JP, Xiao YF. Significant improvement of heart function by cotransplantation of human mesenchymal stem cells and fetal cardiomyocytes in postinfarcted pigs. *Ann Thorac Surg* 74: 1568–1575, 2002.
28. Murry CE, Wiseman RW, Schwartz SM, Hauschka SD. Skeletal myoblast transplantation for repair of myocardial necrosis. *J Clin Invest* 98: 2512–2523, 1996.
29. Orlic D, Kajstura J, Chimenti S, Bodine DM, Leri A, Anversa P. Transplanted adult bone marrow cells repair myocardial infarcts in mice. *Ann NY Acad Sci* 938: 221–229, 2001.
30. Orlic D, Kajstura J, Chimenti S, Limana F, Jakoniuk I, Quaini F, Nadal-Ginard B, Bodine DM, Leri A, Anversa P. Mobilized bone marrow cells repair the infarcted heart, improving function and survival. *Proc Natl Acad Sci USA* 98: 10344–10349, 2001.
31. Pagani FD, DerSimonian H, Zawadzka A, Wetzel K, Edge AS, Jacoby DB, Dinsmore JH, Wright S, Aretz TH, Eisen HJ, Aaronson KD. Autologous skeletal myoblasts transplanted to ischemia-damaged myocardium in humans. Histological analysis of cell survival and differentiation. *J Am Coll Cardiol* 41: 879–888, 2003.
32. Pandian RP, Kutala VK, Parinandi NL, Zweier JL, Kuppusamy P. Measurement of oxygen consumption in mouse aortic endothelial cells using a microparticulate oximetry probe. *Arch Biochem Biophys* 420: 169–175, 2003.
33. Pandian RP, Parinandi NL, Ilango G, Zweier JL, Kuppusamy P. Novel particulate spin probe for targeted determination of oxygen in cells and tissues. *Free Radic Biol Med* 35: 1138–1148, 2003.
34. Parinandi NL, Sharma A, Kuppusamy P. Internalization of particulate spin probe for determination of intracellular oxygen. *Free Radic Biol Med* 35: S148–S148, 2003.
35. Pouzet B, Hagege AA, Vilquin JT, Desnos M, Duboc D, Marolleau JP, Menasche P. Transplantation of autologous skeletal myoblasts in ischemic cardiac insufficiency. *J Soc Biol* 195: 47–49, 2001. [in French.]
36. Schachinger V, Assmus B, Britten MB, Honold J, Lehmann R, Teupe C, Abolmaali ND, Vogl TJ, Hofmann WK, Martin H, Dimmeler S, Zeiher AM. Transplantation of progenitor cells and regeneration enhancement in acute myocardial infarction: final one-year results of the TOPCARE-AMI Trial. *J Am Coll Cardiol* 44: 1690–1699, 2004.
37. Schachinger V, Erbs S, Elsasser A, Haberbosch W, Hambrecht R, Holschermann H, Yu J, Corti R, Mathey DG, Hamm CW, Suselbeck T, Assmus B, Tonn T, Dimmeler S, Zeiher AM. Intracoronary bone marrow-derived progenitor cells in acute myocardial infarction. *N Engl J Med* 355: 1210–1221, 2006.
38. Skud D, Caron N, Goulet M, Roy B, Espinosa F, Tremblay JP. Dynamics of the early immune cellular reactions after myogenic cell transplantation. *Cell Transplant* 11: 671–681, 2002.
39. Smits PC, van Geuns RJ, Poldermans D, Bountioukos M, Onderwater EE, Lee CH, Maat AP, Serruys PW. Catheter-based intramyocardial injection of autologous skeletal myoblasts as a primary treatment of ischemic heart failure: clinical experience with six-month follow-up. *J Am Coll Cardiol* 42: 2063–2069, 2003.
40. Strauer BE, Brehm M, Zeus T, Kostering M, Hernandez A, Sorg RV, Kogler G, Wernet P. Repair of infarcted myocardium by autologous intracoronary mononuclear bone marrow cell transplantation in humans. *Circulation* 106: 1913–1918, 2002.
41. Taylor DA, Atkins BZ, Hungspreugs P, Jones TR, Reedy MC, Hutcheson KA, Glower DD, Kraus WE. Regenerating functional myocardium: improved performance after skeletal myoblast transplantation. *Nat Med* 4: 929–933, 1998.
42. Walter GA, Cahill KS, Huard J, Feng H, Douglas T, Sweeney HL, Bulte JW. Noninvasive monitoring of stem cell transfer for muscle disorders. *Magn Reson Med* 51: 273–277, 2004.
43. Wang JS, Shum-Tim D, Chedrawy E, Chiu RC. The coronary delivery of marrow stromal cells for myocardial regeneration: pathophysiologic and therapeutic implications. *J Thorac Cardiovasc Surg* 122: 699–705, 2001.
44. Weissleder R, Stark DD, Engelstad BL, Bacon BR, Compton CC, White DL, Jacobs P, Lewis J. Superparamagnetic iron oxide: pharmacokinetics and toxicity. *AJR Am J Roentgenol* 152: 167–173, 1989.
45. Winitzky SO, Gopal TV, Hassanzadeh S, Takahashi H, Gryder D, Rogawski MA, Takeda K, Yu ZX, Xu YH, Epstein ND. Adult murine skeletal muscle contains cells that can differentiate into beating cardiomyocytes in vitro. *PLoS Biol* 3: e87, 2005.
46. Wollert KC, Meyer GP, Lotz J, Ringes-Lichtenberg S, Lippolt P, Breidenbach C, Fichtner S, Korte T, Hornig B, Messinger D, Arseniev L, Hertenstein B, Ganser A, Drexler H. Intracoronary autologous bone-marrow cell transfer after myocardial infarction: the BOOST randomised controlled clinical trial. *Lancet* 364: 141–148, 2004.